Supporting Information

V_3S_4/PPy nanocomposites with superior high-rate capability as sodium-ion battery anodes

Yajuan Zhang[a], Yue Li[b], Guangzhen Zhao[a], Lu Han[a], Ting Lu[b], Jinliang Li[c]*, Guang Zhu[a]*, Likun Pan[b]*

[a]*Key Laboratory of Spin Electron and Nanomaterials of Anhui Higher Education Institutes, Suzhou University, Suzhou 234000, PR China.*

[b]*Shanghai Key Laboratory of Magnetic Resonance, School of Physics and Electronic Science, East China Normal University, Shanghai 200241, China.*

[c]*Siyuan Laboratory, Guangdong Provincial Key Laboratory of Nanophotonic Manipulation, Guangdong Provincial Engineering Technology Research Center of Vacuum Coating Technologies and New Energy Materials, Department of Physics, Jinan University, Guangzhou 510632, China*

** Corresponding author: lijinliang@email.jnu.edu.cn (J. Li); lkpan@phy.ecnu.edu.cn (Likun Pan); guangzhu@ahszu.edu.cn (Guang Zhu).*

Material characterizations

The structures of the samples were characterized using various analytical techniques. X-ray diffraction (XRD) patterns were obtained using a D8 ADVANCE PC diffractometer (Bruker, Germany) with Cu/Kα radiation (λ=0.15406 nm). The morphologies of the samples were examined using a Zeiss Ultra 55 field-emission scanning electron microscope (SEM) and a JEOL-2010 transmission electron microscope (TEM). The specific surface areas and pore size distributions of the samples were determined using an Autosorb-iQ analyzer (Quantachrome, USA), and calculated based on the Brunauer-Emmett-Teller multipoint and Barret-Joyner-Halenda models, respectively. X-ray photoelectron spectroscopy (XPS) measurements were performed using a Kratos Axis Ultra instrument with monochromatic Al Kα radiation. The X-ray absorption fine structure (XAFS) spectra were performed at BL11B beamline in SSRF. The beam current of the storage ring was 200 mA in a top-up mode. The V K-edge XAS spectra were recorded at room temperature in the transmission mode, with the ionization chambers filled with N_2. The acquired XAFS data were analyzed by Athena and Artemis software according to the standard procedures.

Electrochemical tests

To prepare the working electrodes, a homogeneous slurry was created by mixing the V_3S_4/PPy active material, Super P, and carboxymethyl cellulose (CMC) in deionized water, with a mass ratio of 6:2:2. This slurry was then coated onto a clean copper foil and dried under vacuum at 120 ºC overnight, resulting in a mass loading of approximately 1.0 mg cm^{-2} of active material on the working electrode. A thin Na plate was used as the counter electrode. The electrolyte consisted of 1 M $NaClO_4$ in a 1:1 w/w mixture of ethylene carbonate and propylene carbonate, with the addition of 5 wt.% fluoroethylene carbonate. The CR2032 coin cells were assembled in an argon-filled glove box with

H_2O and O_2 levels both less than 0.1 ppm. Galvanostatic charge/discharge measurements were performed using a LAND CT2001A battery testing system at a current density of 100 mA g^{-1} in the voltage range of 0.001-3 V, unless otherwise specified. Cyclic voltammetry (CV) curves were recorded using an Autolab electrochemical workstation in a voltage range of 0.001-3 V at a scan rate of 0.2 mV s^{-1}, unless otherwise specified. Electrochemical impedance spectroscopy (EIS) data were measured using the same electrochemical workstation with a perturbation voltage of 5 mV in a frequency range of 0.1 Hz to 0.1 MHz.

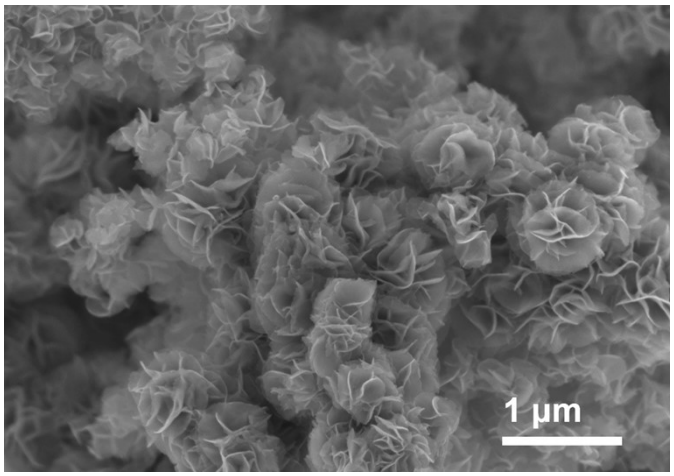

Fig. S1 SEM image of V_3S_4.

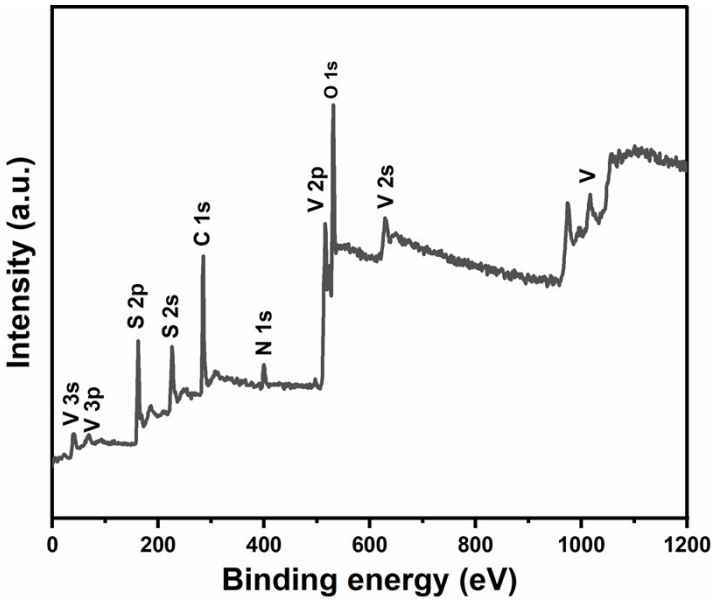

Fig. S2 XPS survey spectrum of VSP-1.

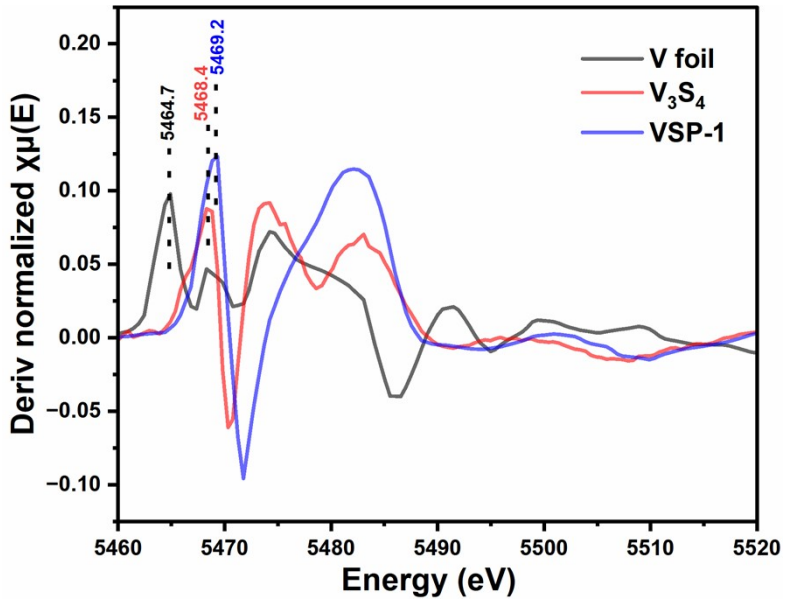

Fig. S3 (a) First-derivative XANES plots for V foil, V_3S_4 and VSP-1 samples.

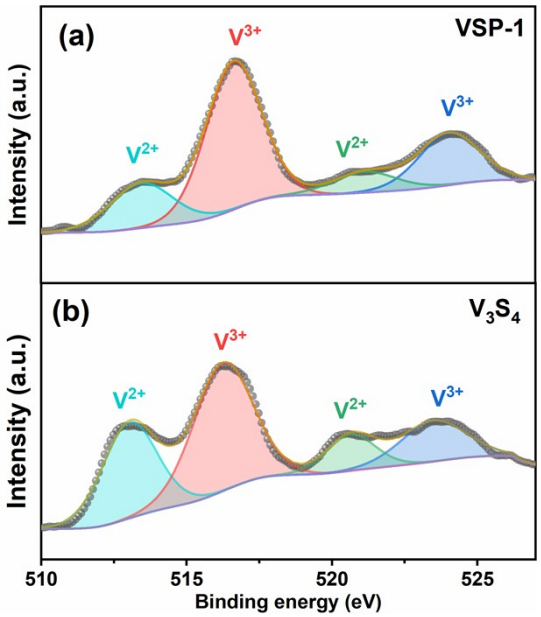

Fig. S4 The high resolution XPS spectra of V_3S_4 and VSP-1 for V 2p.

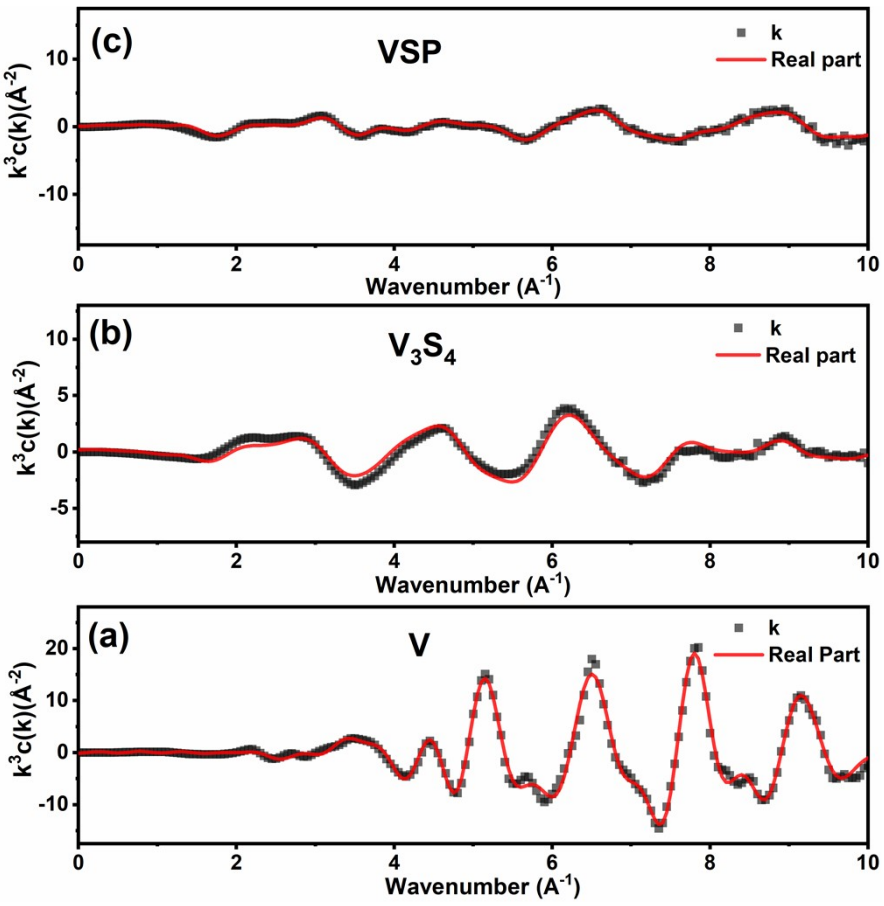

Fig. S5 EXAFS fitting curves of (a) V foil, (b) V_3S_4, and (c) VSP-1 at k space.

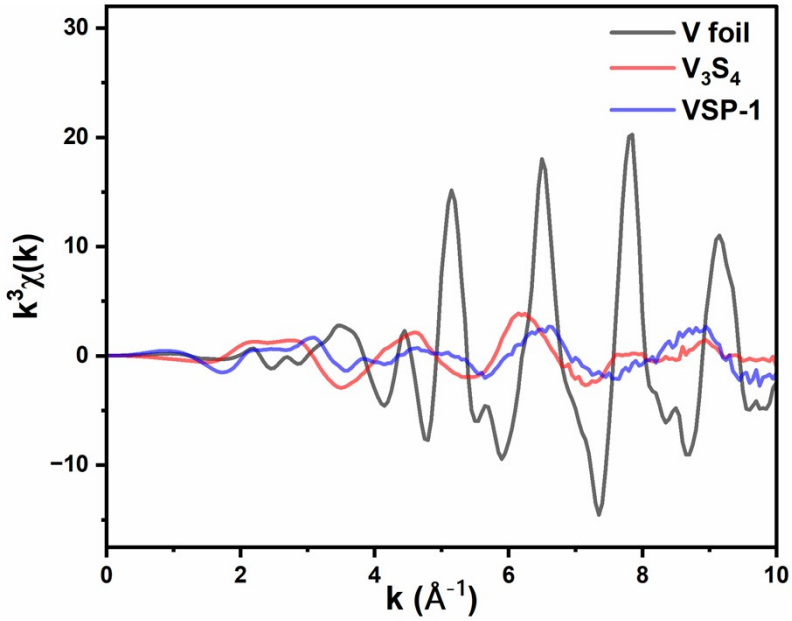

Fig. S6 V K-edge EXAFS curves shown in k^3-weighted k-space for V foil, V_3S_4 and VSP-1 samples.

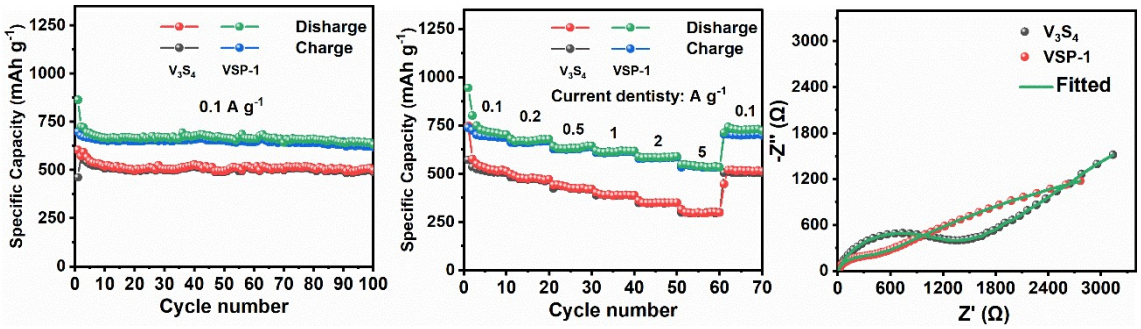

Fig. S7 Cycle performances (a), rate performance (b) and EIS spectra (c) of V_3S_4 and VSP-1.

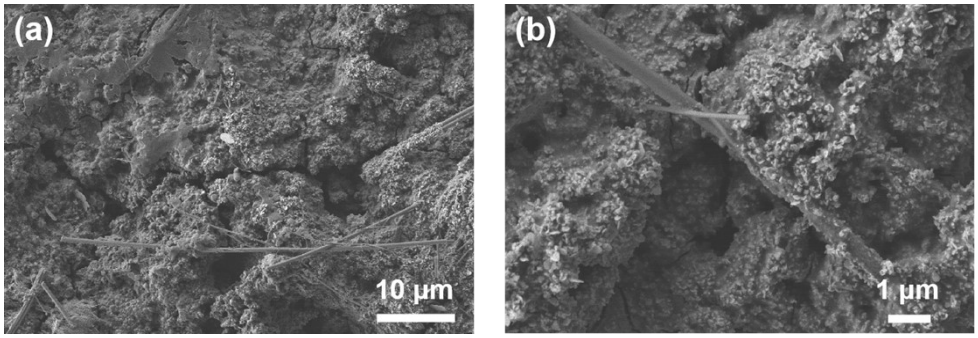

Fig. S8 The FESEM images of VSP-1 electrode after 100 cycles at 0.1 A g^{-1}.

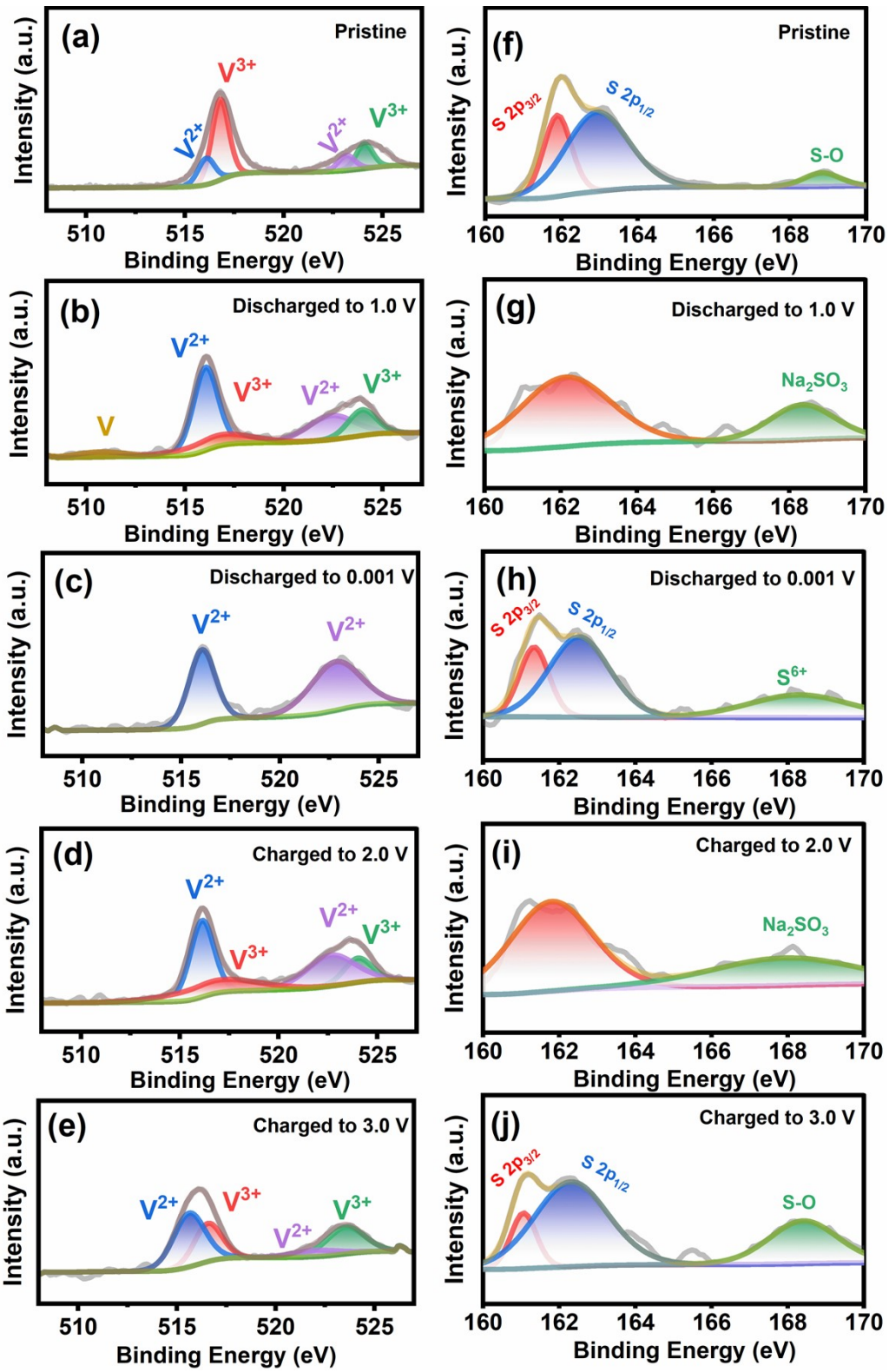

Fig. S9 Ex-situ XPS V 2P (a-e) and S2p (f-j) spectra of VSP-1 in different insertion/extraction states corresponding to the voltage positions in Fig. 5a.

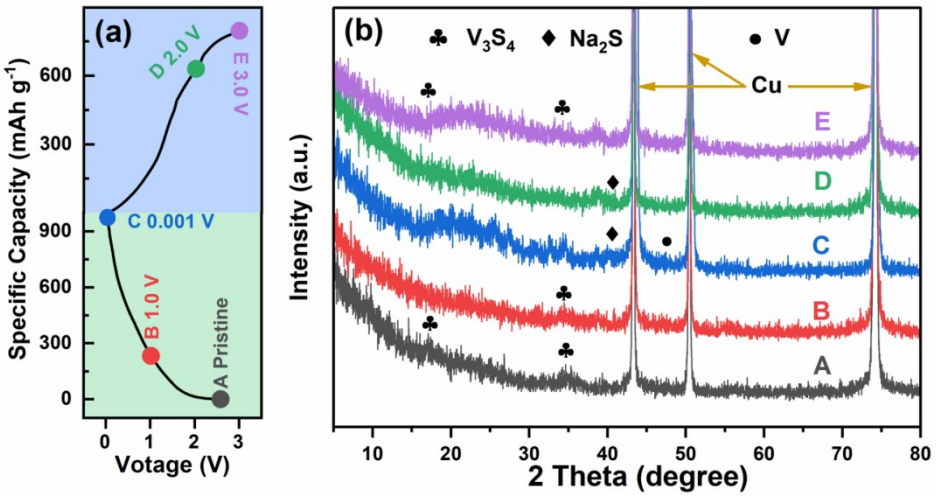

Fig. S10 Ex-situ XRD characterizations of the VSP-1 electrode: (a) discharge/charge curve and the corresponding voltage position, (b) XRD patterns at various states.

Table S1 Pore parameters of VSP-0.5, VSP-1 and VSP-1.5.

Sample	**Specific surface area (m^2 g^{-1})**	**Pore Volume (cm^3 g^{-1})**
VSP-0.5	127	0.228
VSP-1	239	0.562
VSP-1.5	49	0.111

Table S2 Comparison of the sodium-ion storage performances between V_3S_4/PPy in this work and vanadium sulfide-based materials reported in the literatures.

Vanadium sulfide	Initial Coulombic efficiency	Cycling stability	Rate capability	Ref.
VS_2-rGO	56%	350 mAh g^{-1} after 500 cycles at 0.1 A g^{-1}	220 mAh g^{-1} at 1 A g^{-1} 143 mAh g^{-1} at 2 A g^{-1}	[1]

VOOH-VS_2 micro-flowers	82%	330 mAh g^{-1} after 150 cycles at 0.2 A g^{-1}	224 mAh g^{-1} at 1 A g^{-1} 113 mAh g^{-1} at 5 A g^{-1}	2
VS_4@rGO	/	264 mAh g^{-1} after 1000 cycles at 1 A g^{-1}	176 mAh g^{-1} at 5 A g^{-1} 114 mAh g^{-1} at 10 A g^{-1}	3
VS_4-rGO	~75%	237 mAh g^{-1} after 50 cycles at 0.1 A g^{-1}	220 mAh g^{-1} at 0.5 A g^{-1} 192 mAh g^{-1} at 0.8 A g^{-1}	4
VS_4-rGO	~61%	402 mAh g^{-1} after 300 cycles at 0.5 A g^{-1}	340 mAh g^{-1} at 2 A g^{-1} 238 mAh g^{-1} at 5 A g^{-1} 400 mAh g^{-1} at 0.5 A g^{-1}	5
VS_4-rGO	65%	201 mAh g^{-1} after 50 cycles at 0.1 A g^{-1}	309 mAh g^{-1} at 0.8 A g^{-1}	6
VS_4-rGO	71%	463 mAh g^{-1} after 100 cycles at 0.1 A g^{-1}	346 mAh g^{-1} at 1.2 A g^{-1} 270 mAh g^{-1} at 2.4 A g^{-1}	7
VS_4 @ $Ti_3C_2T_x$	81%	599 mAh g^{-1} after 40 cycles at 1 A g^{-1}	/	8
VS_4 @ polydopamine	79%	/	210 mAh g^{-1} at 2 A g^{-1} 173 mAh g^{-1} at 5 A g^{-1}	9

VS_4/carbon nanotube	81%	/	382 mAh g^{-1} at 2 A g^{-1} 368 mAh g^{-1} at 5 A g^{-1}	10
N-doped carbon nanotube@VS_4	82%	430 mAh g^{-1} after 2000 cycles at 1 A g^{-1}	500 mAh g^{-1} at 2 A g^{-1} 460 mAh g^{-1} at 5 A g^{-1}	11
V_5S_8/carbon fiber	49%	462 mAh g^{-1} after 70 cycles at 0.2 A g^{-1}	418 mAh g^{-1} at 1 A g^{-1} 352 mAh g^{-1} at 2 A g^{-1}	12
V_5S_8/carbon fiber	57%	351 mAh g^{-1} after 400 cycles at 0.2 A g^{-1}	210 mAh g^{-1} at 2 A g^{-1} 126 mAh g^{-1} at 5 A g^{-1}	13
V_5S_8-graphite	68%	488 mAh g^{-1} after 500 cycles at 1 A g^{-1}	584 mAh g^{-1} at 1 A g^{-1} 389 mAh g^{-1} at 5 A g^{-1}	14
V_5S_8@Graphene	/	477 mAh g^{-1} after 100 cycles at 1 A g^{-1}	487 mAh g^{-1} at 2 A g^{-1} 432 mAh g^{-1} at 5 A g^{-1}	15
carbon-coated V_2S_3	91%	/	561 mAh g^{-1} at 1 A g^{-1} 484 mAh g^{-1} at 2 A g^{-1}	16
V_3S_4@C nanosheets	40%	578 mAh g^{-1} after 100 cycles at 0.1 A g^{-1}	393 mAh g^{-1} at 1 A g^{-1}	17
V_3S_4@rGO	/	531 mAh g^{-1} after 200 cycles at 0.1 A g^{-1}	287 mAh g^{-1} at 1 A g^{-1} 232 mAh g^{-1} at 2 A g^{-1}	18
V_3S_4@NC	/	166 mAh g^{-1} after 300 cycles at 10 A g^{-1}	307 mAh g^{-1} at 2 A g^{-1} 249 mAh g^{-1} at 5 A g^{-1}	19
V_3S_4@ carbon nanofibers	57%	400 mAh g^{-1} after 400 cycles at 0.1 A g^{-1}	265 mAh g^{-1} at 2 A g^{-1} 200 mAh g^{-1} at 5 A g^{-1}	20

V_3S_4/PPy	79%	619 mAh g^{-1} after 100 cycles at 0.1 A g^{-1}	611 mAh g^{-1} at 1 A g^{-1} 585 mAh g^{-1} at 2 A g^{-1} 535 mAh g^{-1} at 5 A g^{-1}	This work

Reference

1. H. Qi, L. Wang, T. Zuo, S. Deng, Q. Li, Z. H. Liu, P. Hu and X. He, *ChemElectroChem*, 2019, **7**, 78-85.
2. W. Li, J. Huang, L. Feng, L. Cao, Y. Feng, H. Wang, J. Li and C. Yao, *J. Mater. Chem. A*, 2017, **5**, 20217-20227.
3. W. Li, J. Zhang, J. Huang, J. Wang and X. Li, Mater. Lett., 2023, **330**, 133301.
4. R. Sun, Q. Wei, Q. Li, W. Luo, Q. An, J. Sheng, D. Wang, W. Chen and L. Mai, *ACS Appl. Mater. Interfaces*, 2015, **7**, 20902-20908.
5. S. Wang, F. Gong, S. Yang, J. Liao, M. Wu, Z. Xu, C. Chen, X. Yang, F. Zhao, B. Wang, Y. Wang and X. Sun, *Adv. Funct. Mater.*, 2018, **28**, 1801806.
6. L. Zhu, Y. Li, J. Wang and X. Zhu, *Solid State Ionics*, 2018, **327**, 129-135.
7. S. Li, W. He, P. Deng, J. Cui and B. Qu, *Mater. Lett.*, 2017, **205**, 52-55.
8. H. Wang, P. Wang, W. Gan, L. Ci, D. Li and Q. Yuan, *J. Power Sources*, 2022, **534**, 231412.
9. Y. Liu, R. Huang, N. Wei and Y. Zhou, *Ionics*, 2023, **29**, 651-660.
10. P. Yu, S. Xu, K. Yao, H. Yao, W. Yang, X. Lin, H. Yu, W. Liu, Y. Qin and X. Rui, *J. Power Sources*, 2021, **501**, 230021.
11. F. Yang, W. Zhong, M. Ren, W. Liu, M. Li, G. Li and L. Su, *Inorg. Chem. Front.*, 2020, **7**, 4883-4891.

12. L. Xu, X. Chen, W. Guo, L. Zeng, T. Yang, P. Xiong, Q. Chen, J. Zhang, M. Wei and Q. Qian, *Nanoscale*, 2021, **13**, 5033-5044.

13. S. Liu, H. Zhang, M. Zhou, X. Chen, Y. Sun and Y. Zhang, *J. Electroanal. Chem.*, 2021, **903**, 115841.

14. C. Yang, X. Ou, X. Xiong, F. Zheng, R. Hu, Y. Chen, M. Liu and K. Huang, *Energy Environ. Sci.*, 2017, **10**, 107-113.

15. L. B. Tang, P. Y. Li, R. D. Cui, T. Peng, H. X. Wei, Z. Y. Wang, H. Y. Wang, C. Yan, J. Mao, K. H. Dai, H. Z. Chen, X. H. Zhang and J. C. Zheng, *Small Methods*, 2023, **7**, 2201387.

16. L. Shen, Y. Wang, F. Wu, I. Moudrakovski, P. A. van Aken, J. Maier and Y. Yu, *Angew. Chem. Int. Ed.*, 2019, **58**, 7238-7243.

17. Y. Liu, Z. Sun, X. Sun, Y. Lin, K. Tan, J. Sun, L. Liang, L. Hou and C. Yuan, *Angew. Chem. Int. Ed.*, 2020, **59**, 2473-2482.

18. H. Zhang, Y. Zhang, Y. Meng, M. Xiao, J. Hu, G. Zhao, S. Liu and F. Zhu, *Ionics*, 2021, **27**, 5067-5077.

19. Z. Huang, P. Luo, H. Zheng, Z. Lyu and X. Ma, *J. Phys. Chem. Solid.*, 2023, **172**, 111081.

20. G. Yao, P. Niu, Z. Li, Y. Xu, L. Wei, H. Niu, Y. Yang, F. Zheng and Q. Chen, *Chem. Eng. J.*, 2021, **423**, 130229.